

Розглянуто представлення форми дротяної лінії в залежності від натягу проводу і температури. Розроблено метод побудови геометричної тривимірної моделі лінії і синтезу її зображень, який може бути застосовано в системі візуалізації тренажерного комплексу. Вирішення завдання синтезу і візуалізації протяжних об'єктів, є комплексним і обчислювально складним через високу деталізацію таких об'єктів, а також сильну нерівномірність проекції.

Метод дозволяє по відомим параметрам провисання і відстані між точками підвісу отримати набір трикутників, які описують лінію в реальному масштабі часу. Для цього не потрібно проводити сканування лінії на відміну від методів лідарного сканування або фотограмметрії, що застосовуються. Провисання дротів лінії може змінюватися в реальному масштабі часу в залежності від зовнішніх умов. Отриманий набір не містить явно видимих зламів або артефактів для будь-якої позиції спостерігача в межах ділянки лінії що моделюється.

Необхідні обчислювальні ресурси для синтезу зображення лінії мінімізуються за рахунок використання гнучкої системи рівнів деталізації. Така система дозволяє використовувати більш дешеве апаратне забезпечення для побудови системи візуалізації, що веде до зменшення ціни тренажерного комплексу в цілому.

Метод мінімізує артефакти аліасинга на віддалених від спостерігача елементах дротяної лінії, автоматичне накладення текстури і розрахунок нормалей для поверхні лінії, що дозволяє коректно розрахувати освітленість для будь-якого фрагмента лінії при синтезі зображень в системі візуалізації. Проведено оцінку швидкодії методу, його реалізація в рамках системи візуалізації показує швидкодію достатню для роботи в реальному масштабі часу, наведені приклади синтезованих зображень лінії.

Необхідні обчислювальні ресурси для синтезу зображення лінії мінімізуються за рахунок використання гнучкої системи рівнів деталізації. Така система дозволяє використовувати більш дешеве апаратне забезпечення для побудови системи візуалізації, що веде до зменшення ціни тренажерного комплексу в цілому

Ключові слова: БПЛА, провідні лінії, тренажерні комплекси, тривимірні моделі, rasterization, синтез зображень, система візуалізації, графічний прискорювач, аліасинг

DEVELOPMENT OF A METHOD FOR THE SYNTHESIS OF A THREE-DIMENSIONAL MODEL OF POWER TRANSMISSION LINES FOR VISUALIZATION SYSTEMS OF TRAINING COMPLEXES

P. Kachanov

Doctor of Technical Sciences,
Professor, Head of Department*
E-mail: kpa@kpi.kharkov.ua

A. Zuev

PhD, Associate Professor
E-mail: dakarton@gmail.com

*Department of automation and control in technical systems
National Technical University
«Kharkiv Polytechnic Institute»
Kyrpychova str., 2, Kharkiv,
Ukraine, 61002

1. Introduction

Measures are taken to remotely monitor and assess transmission capacity of power transmission line (PTL) networks in countries with large-scale electric power infrastructure such as the USA, the EU [1], China [2], Brazil, [3], RF [4].

The recent level of development of science and technology makes it possible to use fundamentally new methods for solving such problems in addition to classical methods. They include topographic monitoring using unmanned aerial vehicles (UAV) based on visual, thermo-visual and laser scanning of PTLs followed by data processing.

Advantage of such remote monitoring methods consists in possibility of automating and complex monitoring of the transmission line parameters that characterize both external state of the power system objects and its main electrical parameters.

In this case, the use of UAVs, especially in automatic mode, requires careful study of routes and flight tasks. As a result, requirements to quality of their management grow which requires grading up the qualitative level of operators training. Training of operators and working out of flight tasks with a direct operation of UAVs on power lines is expensive and not always possible. In this case, activity of undertrained operators can lead both to the UAV failures because of accidents and, accordingly, to expensive repairs and the consequences posing a threat to people's lives. Thus, it is advisable to use simulation and training complexes (STC) which use computer synthesis of environment in the process of training and modeling. Such complexes lack disadvantages of conventional training methods, have a low cost of both the complex itself and its operation, are safe for people and enable simulation of any situations that arise during operation of a UAV in the monitoring process.

Visualization system (VS) is the key component of the STC applying computerized synthesis of environment. The system makes it possible to provide the operator with the UAV control principles, allows him to respond quickly to various situations arising during the flight task simulation. It shows the results of his actions and enables monitoring and evaluation of the training process [5]. The base part of the VS-STC is the process of modeling the environment visible to the operator in the most realistic way using tools, methods and algorithms of computer graphics.

Urgency of the studies is determined by impossibility of effective solution of monitoring problems without preliminary modeling using the STC the key part of which is the VS. At the same time, existing algorithms and methods for image synthesis in VS do not make it possible to realistically represent wire PTLs.

2. Literature review and problem statement

Since their appearance, the UAVs were used mainly for military purposes. But the cheaper hardware has resulted in their greater availability as remote sensing tools [6]. They are used in such areas as precision farming, observation of landslides or communications. For example, the problem of detecting road surface damage was solved in [7] by means of stereoscopic survey of the roadway with subsequent obtaining of its three-dimensional model. However, despite the rather high accuracy of the model of roadway surface (about 5 mm) the method proposed cannot be used to obtain models of objects having spatial structure and located at several levels above the land. In addition, the optical system itself is mounted on the UAV rigidly which makes it difficult to photograph at varied angles. The resulting surface texture also contains a luminance component which is typical for all methods of photogrammetry. Therefore, application of the model reconstructed in this way directly in the VS-STC system is difficult since it is necessary to remove glares and shadows that negatively affect both quality of spatial reconstruction (as indicated in the work) and subsequent calculation of illumination during visualization.

Another widely used procedure for obtaining three-dimensional models of real objects, i.e. lidar scanning, was considered in [8, 9]. Such scanning makes it possible to obtain clouds of points that describe three-dimensional objects spatially and provide with information on their surface characteristics. Based on the resulting cloud, a grid of triangles is created which is then used for further modeling and visualization of the object. Disadvantages of this method include relatively low resolution (of the order of units of meters). Even though resolution can be raised to tens of centimeters with the help of a number of improvements proposed in these works, this is not enough to obtain a wire line model. At the same time, the equipment used in this technique (lidars) is very expensive and heavy. This imposes restrictions on the size of the UAVs used and raises cost of the entire system. It should be noted that lidar scanning does not create a surface texture of the object which complicates calculation of illumination. On the other hand, reflective characteristics of the object surface are determined which makes it possible to simplify classification and separation of objects in the models obtained.

Paper [10] demonstrates application of UAV in archaeology with a three-dimensional reconstruction of the field of interests at theoretical accuracy of object localization about 0.6 cm horizontally and 2.3 cm vertically. However, similarly to [7], this method works with objects located at nonintersecting altitudes and in small areas (up to 100 m²). For scanning of non-planar objects, it was suggested to make several successive flights which in general significantly increases time and complicates the process of model construction. Although there are realizations of such algorithms, for example in [11], which make it possible to improve accuracy (by 40–50 %) of the obtained models and slightly speedup scanning, they do not solve the problem in general. In addition, the use of specialized algorithms of navigation and positioning of the UAV cameras requires the use of expensive and high-speed equipment on board the UAV.

It was pointed out in [12] that the accuracy of lidar scanning is poor. It allows one to restore shape, even for objects of large size, such as trees but just partially. Theoretical possibility of using cameras working in the visible range for recognizing large fragments of objects on the obtained three-dimensional model was shown in this paper. At the same time, the confidently recognized fragments have dimensions considerably exceeding section of the line cable. Besides, the proposed method requires a complex flying trajectory around the object to obtain its model which is not always possible for a wire line because of overgrowing of the PTL corridors and uncertainty in location of wire within the line because of its sagging.

The method of obtaining panoramic images of real objects which can be used for texturing in VS was considered in [13]. Similar to [7], a high-resolution camera working in a visible light range was used as a data source. The method features photographing with a substantial overlap and positioning of the obtained frames using both a satellite navigation system and a theodolite. This greatly complicates the process of model construction. In this case, accuracy of determining coordinates of objects on the landscape surface is about 5 mm horizontally and 17 mm vertically. The paper demonstrates an example of using this method to obtain the terrain surface textures. However, this method does not ensure obtaining of a spatial shape of the object corresponding to the texture.

Factors that affect accuracy of photogrammetric (and lidar) methods for constructing three-dimensional models of real objects with the help of UAVs were considered in [14]. They include weather conditions and insufficiently accurate data provided by a positioning system. A method for estimating and analyzing the errors that arise in solving this problem was also considered. Principal impossibility of excluding a number of errors in determining coordinates of the objects obtained by photogrammetric methods was shown. In this case, the practical study carried out in the work used the same distances (2–5 km) and altitudes (less than 200 m) that are typical for monitoring wire PTLs.

A common drawback of the methods used is the need for a complex procedure of obtaining the object images and the use of expensive equipment. Disadvantages are the same: insufficient accuracy of the three-dimensional models obtained and lack of guarantees of obtaining a complete closed model, especially for complex composite objects. In addition, most of the known algorithms give a "cast" of the model at a certain time moment which makes it practically impossible to vary the model shape and parameters in real time. This is

because of objective complexity of automatic division of the composite model into sections as well as long (up to several days) and resource-intensive process of obtaining a three-dimensional model itself.

On the other hand, to solve the problems facing the imitation and training complexes, it is necessary to change parameters of the three-dimensional model depending on the nature of the modeling processes and the tasks performed. The models of three-dimensional objects obtained by the photogrammetric method and lidar scanning do not fully satisfy this requirement.

It should also be noted that the issues of texturing and lighting calculation as well as realistic visualization of the obtained models were practically not considered. The applied methods were destined to work with flat or laying at the same level spatial structures (forests, landscapes, roads). The methods for obtaining three-dimensional models of complex industrial facilities such as wire PTLs and other objects of energy infrastructure have not been investigated sufficiently enough.

It should also be noted that the models obtained by photogrammetry methods are highly detailed and cannot be applied directly to VS-STC. This is because visualization requires significant computational capabilities.

In this regard, there is a need of developing a method for obtaining a three-dimensional model of a wire PTL and synthesis of its image. It is expedient to base this model on the analytical representation of a wire line. This will enable its use for VS of simulation and training modeling in various external conditions.

3. The aim and objectives of the study

This work objective was to develop a method for construction of a three-dimensional model of a wire PTL that could be used to synthesize images in VS-STC using 3D graphics accelerators.

To achieve the objective, the following tasks were set:

- to analyze features of representing models of extended objects with one of the overall dimensions significantly exceeding the others;
- to develop a mathematical description of the wire power line model and a method for obtaining its geometric representation and visualization using computer graphics tools;
- to substantiate the possibility of using the proposed method for image synthesis in real time for various values of wire sagging.

4. Analysis of features of representation of wire lines

Let us consider analytical models of a wire line used in calculating parameters of PTLs [15–19].

The most important characteristic of a PTL is the shortest vertical distances from its wires to nearby structures that must be observed under various weather and climatic conditions (Fig. 1).

Mechanical stresses and wire sags vary with temperature and load [15]. When temperature grows, the wire lengthens resulting in the sag increase and a stress decrease in the wire.

The stress changes in the wire caused by changes of atmospheric conditions are described by the following equation of the wire state [16]:

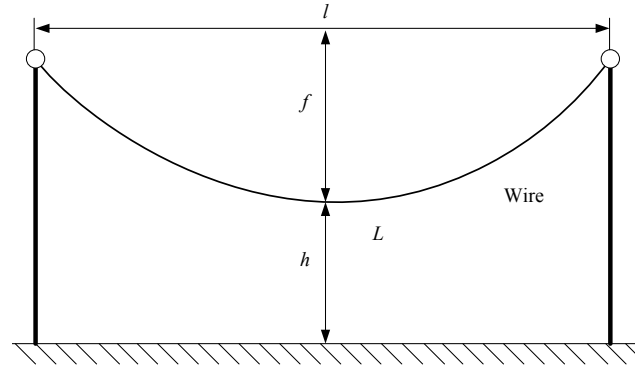


Fig. 1. Diagram of vertical dimensions of PTL

$$\sigma_i - \frac{\gamma^2 \cdot E \cdot l^2}{24 \cdot \sigma_i^2} = \sigma_0 - \frac{\gamma_0^2 \cdot E \cdot l^2}{24 \cdot \sigma_0^2} - \alpha \cdot E \cdot (t_i - t_0), \quad (1)$$

where σ_0 , σ_i is stress in the wire (MPa) at the initial time and at the time of measurement, respectively; γ is the specific load from the wire weight, MPa/m; E is the modulus of elasticity of the wire material; l is the wire length, m; α is the coefficient of linear expansion of the wire material; t_0 is temperature at the initial time moment; t_i is temperature at the time of measurement.

Tensile stress in the wire can be determined as

$$\sigma = \frac{T}{d}, \quad (2)$$

where T is the tensile force (tension in the wire), H; d is the wire cross-section, mm².

Expression (1) determines size of the sag according to the known initial state and temperature change. The curve of sagging of a wire fixed to suspensions at both ends at the same level can be approximated by the equation [17]

$$f = \frac{\gamma \cdot l^2}{8 \cdot \sigma} + \frac{\gamma^3 \cdot l^4}{384 \cdot \sigma^2}. \quad (3)$$

Total length of wire

$$L = l \cdot \left(1 + \frac{\gamma^2 \cdot l^2}{24 \cdot \sigma^2} \right). \quad (4)$$

When applying load, $T_i = \sigma_i \cdot d$ (2), the total wire length will be equal to

$$L_i = L_0 \cdot (1 + \alpha \cdot t_i) \cdot (1 + \beta \cdot \sigma_i), \quad (5)$$

where $\beta = 1/E$ is the coefficient of elastic elongation of the wire material, mm²/N.

According to [18], it is necessary to take into account significant errors in calculation of long spans or at significant differences in the altitude of the power line supports (topography) as a limitation of applicability of the "classical" method for calculating parameters of a wire line. It is also advisable that calculations take into account the difference in locations of the wire suspensions along the vertical axis (Fig. 2). Then, according to [19], equation of the wire sag curve takes the form:

$$y(x) = \varepsilon \left(\operatorname{ch} \frac{x - x_0}{\varepsilon} - 1 \right) + y_0, \quad (6)$$

where ε is the parameter that determines shape of the sag curve; (x_0, y_0) are coordinates of the lowest wire point;

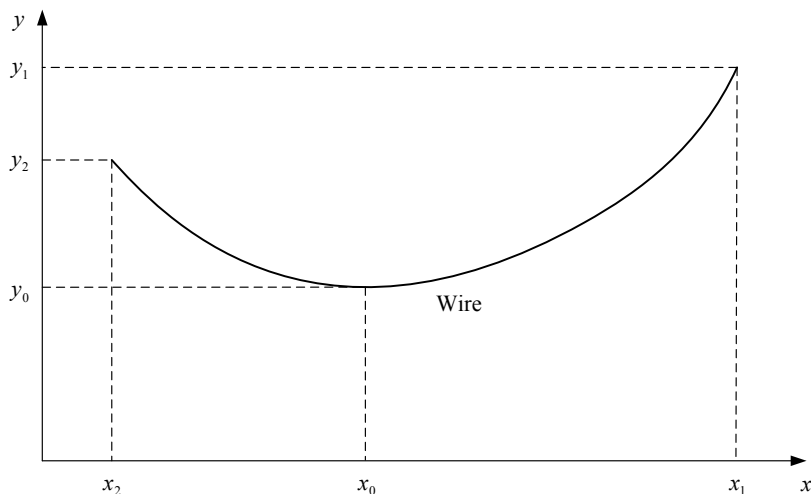


Fig. 2. Diagram of vertical dimensions of PTL taking into account different heights of suspensions

The value of x_0 is

$$x_0(\varepsilon) = \frac{x_1 + x_2}{2} - \varepsilon \cdot \ln\left(\phi(\varepsilon) + \sqrt{\phi(\varepsilon)^2 + 1}\right) \tag{7}$$

where

$$\phi(\varepsilon) = \frac{y_1 - y_2}{2 \cdot \varepsilon \cdot \operatorname{sh}\left(\frac{x_1 - x_2}{2 \cdot \varepsilon}\right)}, \quad \operatorname{sh} x = \frac{e^x - e^{-x}}{2}$$

The total length of the wire will be [18]

$$L(\varepsilon) = 2 \cdot \varepsilon \cdot \operatorname{ch}\left(\frac{x_1 + x_2 - 2 \cdot x_0(\varepsilon)}{2 \cdot \varepsilon}\right) \cdot \operatorname{sh}\left(\frac{x_1 - x_2}{2 \cdot \varepsilon}\right) \tag{8}$$

The amount of wire sag at a point with coordinates (x, y) can be defined as

$$f(\varepsilon, x) = \tilde{\varepsilon} \cdot \left[\operatorname{ch}\left(\frac{x_2 - x_0(\varepsilon)}{\tilde{\varepsilon}}\right) - \operatorname{ch}\left(\frac{x - x_0(\varepsilon)}{\tilde{\varepsilon}}\right) \right], \tag{9}$$

where $\tilde{\varepsilon} = \varepsilon \cdot x_2$.

According to [20], elongation of the wire from heating by solar radiation can be approximated by the expression

$$\Delta l_{sum} = \alpha \cdot l \cdot (t_i - t_0) \tag{10}$$

Accordingly, the change in the amount of wire sag will be linearly dependent on Δl_{sum}

$$\Delta f_{sum} = \frac{\Delta l_{sum}}{K} = \frac{\alpha \cdot l \cdot (t_i - t_0)}{K}, \tag{11}$$

where $K \approx 3,42$ is the empirical coefficient when temperatures change $\Delta t = 2 \dots 12$ °C.

The total wire sag for temperature t_i will be

$$f_i = f_0 + \Delta f_{sum} \tag{12}$$

5. Mathematical model of a wire line

In order to apply expressions (7), (9) in constructing a line model in three-dimensional space, represent the PTL as a piecewise linear function. Superpose direction of each segment with the x-axis (Fig. 2). In this case:

$$l = \sqrt{(x_1 - x_2)^2 + (z_1 - z_2)^2}, \tag{13}$$

where x_i, z_i are the coordinates of the point of suspension in a plane parallel to the plane of the earth's surface.

It is advisable to shift the origin of the coordinate system to one of the points of suspension beginning and represent the values in the x-axis in a relative form taking $(x_1 - x_2)/l = 1$, then $x'_1 = 0, x'_2 = 1$, in the suspension points:

$$A = \{x_1, y_1, z_1\}, \quad B = \{x_2, y_2, z_2\}$$

Expression (9) takes the following form

$$f(\varepsilon, x') = l \cdot \varepsilon \cdot \operatorname{ch}\left(\frac{1 - x'_0}{\varepsilon}\right) - l \cdot \varepsilon \cdot \operatorname{ch}\left(\frac{x' - x'_0}{\varepsilon}\right), \tag{14}$$

where $x' = x/l, x'_0 = x_0(\varepsilon)/l$.

The augend in expression (14) does not depend on x and can be calculated once before calculation of the line begins. To obtain the line coordinates for each PTL section, the following algorithm is used:

- 1) the value of l is calculated according to (10);
- 2) $x_0(\varepsilon)$ and the corresponding x'_0 are calculated;
- 3) constant summand $l \cdot \varepsilon \cdot \operatorname{ch}\left(\frac{1 - x'_0}{\varepsilon}\right)$; is defined
- 4) $P = A$;
- 5) $s = 0 \dots l$, with step t ;
- $x' = (s + t)/l, P' = x' \cdot B + (1 - x') \cdot A$;
- $P'_y = P'_y - f(\varepsilon, x')$;
- create segment $\{P, P'\}$;
- $P = P'$.

The line in the STC modeling system is represented as a set of nodes (supports) and the topology of their connection. Each line is assigned a unique identifier that makes it possible to dynamically load the line parts located in different parts of landscape and uniquely determines their connection. The active (loaded) nodes of the lines are ordered in ascending order of identifiers. For nodes with the same line identifier, ordering is performed remotely depending on the distance from any of the end nodes. This ensures correct sequence of nodes in the line. Since the nodes in the line are arranged in series, one may choose not to save topology of their connections.

Each node has several connection points (wires, lightning ropes) which must be connected in corresponding lines. To obtain each line, it is necessary to determine position and orientation of the node in the world coordinate system for each pair of neighboring nodes, then determine position of the connection point by translating its coordinates from the local system (relative to the support) to the world system. According to (13), we proceed to representation of the line in

which the axis connecting two nodes will coincide with the x -axis in the diagram of vertical dimensions of the PTL wire (Fig. 2). Further, sag is calculated for each line according to (14) taking into account temperature (10) with a constant step $\Delta x = 1$. Thus, a set of points will be obtained that approximate the line with some small inaccuracy depending on the step and the ε value. Use of such a sequence for geometry synthesis is impractical for the visualization system in view of redundancy of the points, even at a small distance (50 m) from the observer.

It is advisable to simplify line representation in such a way that representation of the line wire in a form of segments at any distance from the observer is unnoticeable. Analysis of the chain line shape (Fig. 2) allows one to conclude that the most noticeable shape distortions introduced by "linearization" will be in the locations where the wire sag is greatest (the greatest tangent inclination angle). At the same time, as distance from the observer increases, $z \rightarrow \infty$, noticeability of distortion decreases proportionally to $1/z$.

Another problem that occurs when visualizing wire lines consists in a significant anisotropy of their dimensionality (thickness is much less than length) which leads to appearance of aliasing effects, even at insignificant distances from the observer when projection of the wire thickness becomes smaller than the pixel size in the synthesized image. This, in turn, leads to a variety of visual artifacts (flickers, line fragmentation) alien to the picture observed during the UAV operation. To reduce such artifacts, it is advisable to draw the line fragments as a line, rather than a grid of triangles, with thickness less than a certain value, smoothly reducing their noticeability when they move away from the observer.

Thus, it is necessary to develop a procedure for changing (selecting) the levels of detail by three criteria:

- 1) noticeability of linearization distortions as a function of distance from the observer;
- 2) size of projection of the line wire diameter on the image;
- 3) minimization of the number of primitives (triangles, line segments) which form the line model.

Let us establish criterion for distortions in linearization as the angle of the line fragment inclination

$$k_l = \arctg \frac{\Delta h}{\Delta x}, \quad (15)$$

where $\Delta h = \Delta y$ (Fig. 2) is the height difference between two points of the line; Δx is the distance between two line points along the x -axis of a horizontal line.

The criterion k_d for the size of projection of the line wire diameter in the image is obtained knowing that the size of the object projection is equal to

$$p = \frac{(d/z) \cdot h}{2 \cdot \text{tg} \frac{fov_y}{2}}, \quad (16)$$

where fov_y is the vertical viewing angle; d is the wire diameter; h is the height of the synthesized image in pixels.

Let us assume that $k_d = f(z)$. Then it follows from (16) that

$$k_d = \frac{d \cdot h}{2 \cdot p \cdot \text{tg} \frac{fov_y}{2}}. \quad (17)$$

Choose the value of p as

$$p = \frac{\sqrt{d^2 + d^2}}{d} = \sqrt{2},$$

in order to take into account the cases when the line projection in the image is positioned at an angle close to 45° to the pixel grid.

The criterion for minimizing the number of primitives forming the line is not specified explicitly but is obtained from the abovementioned two criteria which minimize the number of points in the line (15) or the number of primitives required to represent the line fragment (17). Both criteria can be calculated in advance: k_l at the stage of constructing the line model and k_d before the start of the image synthesis since it depends only on the shape of the observer's field of view and the size of the synthesized image which do not change during the frame synthesis.

To ensure maximum speed of the line geometry synthesis function which is performed before it is rendered in each frame, it is advisable to create l_{\max} sets of points (levels of detail) with the k_l value consistently increasing in each of them. Thus, the problem will be reduced to selection of the necessary detail level, l , for each line fragment (connection between nodes) depending on the z_{\min} magnitude, i. e. the distance between the observer and the nearest point in the line fragment. Proceeding from the assumption that the wire is located along the horizontal axis of the PTL without significant deviations, this quantity is defined as $\min\{z_0, z_{n/2}, z_n\}$, i. e. a minimum from the distances to the end points of the segment and the midpoint (or the point with the maximum sag).

The choice of the type of the primitives forming the line section is defined as follows:

$$\begin{aligned} \text{line} &= z_{\max} > k_d, \\ \text{tri} &= (z_{\min} < k_d) \vee (l < l_t), \end{aligned} \quad (18)$$

where line is the attribute of drawing with line segments; tri is the attribute of drawing with a grid of triangles;

$$z_{\max} = \max\{z_0, z_{n/2}, z_n\},$$

where $l_t = \beta \cdot l_{\max}$ is the threshold of detail level; $\beta = 0, 2 \dots 0, 5$ is the detail factor that allows one to adjust smoothness of transition between representation of the wire in a form of triangles or line segments.

The line and tri attributes overlap which makes it possible to realize a smooth seamless transition between different representations by means of some redundancy (1-2 line fragments) during rendering.

6. Method for obtaining a geometric line representation

To obtain geometric representation of a line in the UAV's VS-STC using the key points of the chosen set l , it is necessary to construct a set of vertices and indices to describe their connections. This set will be loaded into the graphics accelerator and rasterized using the specified firmware.

To represent in a form of line sections (Fig. 3), the set of vertices, V , will exactly coincide with the set of the line points and the set of indices (primitives) can be obtained as

$$P_k = \{v_k, v_{k+1}\} \text{ for } k=0..m-1, \tag{19}$$

where v is the number of the vertex in V ; m is the number of points in the selected set, l .

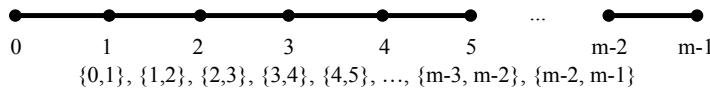


Fig. 3. Representation of a fragment as the line sections

The fragment is continuous, so indices of the vertices coincide for adjacent primitives.

To represent a fragment in a form of a grid of triangles, it is necessary to synthesize a circle for each point and connect adjacent circles in a way providing a cylinder with diameter equal to the wire diameter (Fig. 4).

In order to convey appearance of the wire line taking into account illumination parameters specified in VS-STC, it is necessary to calculate the normal to the surface of the cylinder and two-dimensional texture coordinates to obtain the wire surface properties discretized and recorded in the texture.

Let us establish that each circle consists of s segments of the same size. Then one can obtain an offset from the line center for each point of the circle as

$$\mathbf{n} = \{-\sin \phi, \cos \phi, 0\}, \tag{20}$$

where $\phi = \frac{2 \cdot \pi}{i}$ is the angle of rotation of a point in a unit circle, $i=0..s$.

The coordinates of the circle point with allowance for (20) are defined as follows

$$C_i = N \cdot \frac{d}{2} + A, \tag{21}$$

where A is the coordinates of the point from the l set; $N = \mathbf{B} \cdot \mathbf{n}$ is the normal to the wire surface in the world space; \mathbf{B} is a 3×4 matrix for transition from the local space (Fig. 2) of the PTL fragment to the world space of the VS-STC.

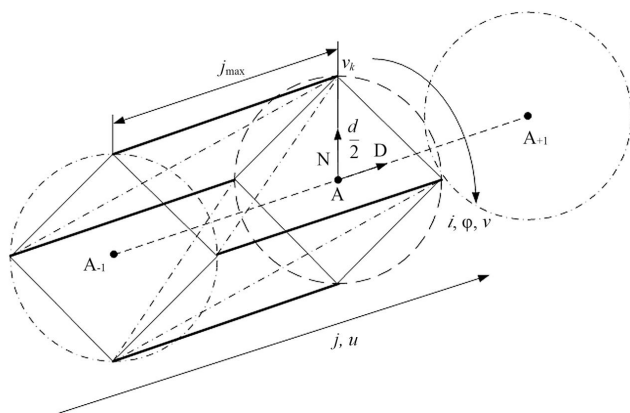


Fig. 4. Representation of a fragment of a line in the form of a grid of triangles

The matrix \mathbf{B} can be obtained from two adjacent points of the line, A and A_{+1} , which specify its direction

$$D = \|A_{+1} - A\|. \tag{22}$$

To obtain rows of the matrix (of orthogonal vectors perpendicular to D in the 3×3 domain and the origin offset)

$$\mathbf{B} = \begin{bmatrix} T_x \\ T_y \\ D \\ A \end{bmatrix}, \tag{23}$$

where

$$T_y = \|D \times T_x\|;$$

$$T_x = \begin{cases} \{-D_z, D_y, D_x\}, & \text{if } |D_z| > |D_y|, \\ \{-D_y, D_x, D_z\}, & \text{if } |D_z| \leq |D_y|. \end{cases}$$

A pair of texture coordinates $\{u, v\}$ is defined as follows:

$$u = s_u \cdot \sqrt{D \cdot D},$$

$$v = i/s, \tag{24}$$

where $s_u = 0,25..4,0$ is the coefficient specifying frequency of repetitions of the texture pattern depending on the line length (a higher value gives a higher repetition frequency).

For the u coordinate, when selecting the texture, it is necessary to enable the repeat mode in which the integer part of the coordinate will define the repeat number. For v , the values do not leave the range $0..1$, so any sampling mode (repeat or limit) can be used.

The set of indices (primitives) consists of number triples (triangles are used) and can be obtained for even triangles

$$P_{k0} = \{v_k + j - j_{\max}, v_k + j, v_k + j_{+1}\},$$

for odd triangles

$$P_{k1} = \{v_k + j_{+1}, v_k + j_{+1} - j_{\max}, v_k + j - j_{\max}\}, \tag{25}$$

where j_{\max} is the number of segments forming a circle; j is the current segment; v_k is the number of the first vertex forming the circle

$$j_{+1} = \begin{cases} j+1, & \text{if } j+1 < j_{\max}, \\ 0, & \text{if } j+1 = j_{\max}, \end{cases} \quad j=0..j_{\max}-1. \tag{26}$$

Expression (26) makes it possible to seamlessly close the cylinder which approximates the wire line surface. The triples of the triangle indices obtained according to (25) are oriented clockwise and form outer surface of the cylinder. The resulting geometric description of the line does not contain clearly visible kinks or artifacts for any position of the observer within the line section modeled in the STC.

Because of geometry specificity of the wire lines (a dimension on one of the coordinate axes considerably exceeds dimensions on the other axes), even at a small distance from the observer, the line projection will have thickness less than the pixel size. This feature requires special processing of the deleted line fragments. Since it is impossible to correctly visualize objects with dimensions less than a pixel in the image, filtering by various methods is used in practice. Its main principle is the change of color of such fragments depending on their thickness. Such a filter can be described as follows

$$c' = (1 - \alpha) \cdot c + \alpha \cdot c_b, \quad (27)$$

where c' is the displayed pixel color; c, c_b are the line and background colors, respectively; $\alpha = f(d_v)$ is the filtration coefficient dependent on the distance between the line fragment and the observer.

Thus, the problem reduces to calculating the α value and determining the background color, c_b . The α quantity is calculated in the vertex firmware synthesizing geometry of the wire line according to the following expression:

$$\alpha = \min \left(1, \frac{\max(0, d_v - d_{\min})}{d_{\max} - d_{\min}} \right), \quad (28)$$

where d_{\min} is the distance from the observer at which the line size becomes less than the pixel size (which is calculated according to the expression (17); d_{\max} is the distance from the observer at which the line cannot be drawn.

The resulting α value lies in the range from 0 to 1 and is stored in one of the channels of the G-buffer [21] formed for the delayed illumination calculation and then used to calculate the resulting color. The synthesized image is superimposed on a full-screen filter:

$$c'(x, y) = \begin{cases} c(x, y), & \text{if } G_\alpha = 0, \\ c(x, y) \cdot (1 - G_\alpha) + c_b(x, y) \cdot G_\alpha, & \text{if } G_\alpha > 0, \end{cases} \quad (29)$$

where G_α is the value of a quantity calculated according to (29) and placed in the G-buffer; (x, y) are pixel coordinates on the screen.

To determine the $c_b(x, y)$ value, the following procedure is used. Colors of all pixels in the vicinity of a pixel with (x, y) , coordinates for which the following inequality is satisfied are selected

$$d_i > d(x, y) + b, \quad (30)$$

where $d(x, y)$ is the distance from the observer for the pixel with (x, y) ; coordinates; d_i is the distance from the observer to the pixel in vicinity of (x, y) ; $b = 0, 1, \dots, 2, 0$ is some empirically chosen threshold that divides background and objects in the image.

All pixel colors satisfying (30) are summed with the weight coefficients and the resulting sum is normalized and used as the background color in expression (29)

$$c_b(x, y) = \frac{1}{\sum_{d_i > d(x, y) + b} w_i} \sum c_i \cdot w_i, \quad (31)$$

where w_i is the pixel weight coefficient; w_0 is the sum of all coefficients for the pixels satisfying condition (30).

7. Results obtained in the experimental study

Quantitative characteristics of the line model for various ε values are given in Table 1.

Program implementation of the proposed method was performed in C++ language and a study of its performance characteristics was performed. The API Direct X was used as a basis for functioning of the VS-STC. The images were synthesized using the ATI Radeon 7770 graphics accelerator. The performance was tested on a system running in Windows OS and equipped with a 32 GB RAM, an Intel Core i7 6700 processor running at 3.4 GHz. A ~12 km section of the 330 kV PTL between Yakivlivka and Konstantivka villages (Kharkiv region, Ukraine) and the landscape at a distance of up to 4 km from the PTL were taken as a basis for modeling. The frame rate in the VS-STC was fixed at a level of 30, the size of synthesized images was 2,560×1,080. To calculate illumination, a method of delayed lighting using the G-buffer and the α value was entered in one of its channels. Examples of images synthesized by the VS-STC according to the proposed method are shown in Fig. 5.



Fig. 5. Examples of a wire line images synthesized according to the proposed method at various observer positions

Table 1

Quantitative characteristics of the line for various ε values

ε	Span 1		Span 2		Span 3	
	Span length, m	Sag, m	Span length, m	Sag, m	Span length, m	Sag, m
10	252.21	3.22	365.25	4.58	446.29	5.58
9	257.23	3.58	365.29	5.09	446.33	6.20
8	257.27	4.02	365.34	5.72	446.39	6.98
7	257.32	4.60	365.41	6.54	446.48	7.98
6	257.40	5.37	365.52	7.63	446.61	9.31
5	257.53	6.44	365.70	9.16	446.84	11.17
4	257.77	8.05	366.05	11.46	447.26	13.97
3	258.29	10.75	366.78	15.29	448.16	18.65
2	259.78	16.17	368.89	23.00	450.74	28.05
1	267.91	32.85	380.40	46.74	464.85	56.98

Dependence of the number of line segments for various detail levels on the parameter (sag magnitude) is given in Table 2.

Table 2

Dependence of the number of segments on ε

ε	Level 1	Level 2	Level 3	Level 4
10	45	27	15	10
9	49	28	15	10
8	56	31	15	11
7	64	35	20	11
6	75	40	23	14
5	88	46	27	15
4	108	59	32	16
3	142	76	40	23
2	186	109	59	31
1	366	184	107	56

The length of the segment between suspensions was 366.2 m, initial number of segments was 369. On average, the optimization time for 369 segments was 42 μ s.

The graph of the number of line segments for various detail levels vs. the sag value, ε , is given in Fig. 6.

The ratio of primitives in the optimized line for various detail levels to that of the original line (without optimization) is shown in Table 3.

The number of triangles, c_Δ , and vertices, c_v , forming a line is linearly dependent on the number of segments and is determined as follows:

$$c_\Delta = c_s \cdot (2 \cdot j_{\max}),$$

$$c_v = (c_s + 1) \cdot j_{\max}, \tag{32}$$

where c_s is the number of segments in the line.

As can be seen from Table 3, after optimization, at the last level of detail, the number of primitives at the maximum sag did not exceed 2 % of the original fragment.

Table 4 shows performance indicators of the method for two lines.

Table 3

Optimization level

ε	Level 1	Level 2	Level 3	Level 4
10	0.122	0.073	0.041	0.003
9	0.133	0.076	0.041	0.003
8	0.152	0.084	0.041	0.004
7	0.173	0.095	0.054	0.004
6	0.203	0.108	0.062	0.005
5	0.238	0.125	0.073	0.005
4	0.293	0.160	0.087	0.005
3	0.385	0.206	0.108	0.008
2	0.504	0.295	0.160	0.011
1	0.992	0.499	0.290	0.019

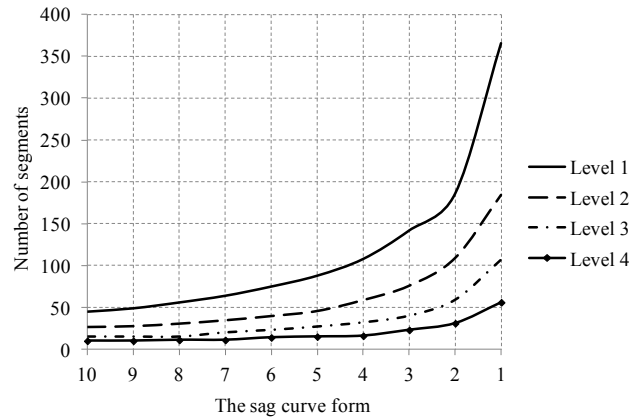


Fig. 6. Dependence of the number of segments on

Table 4

Time of synthesis of the line fragments

No.	Line 1			Line 2		
	Length, m	Synthesis time, μ s	Synthesis speed, km/s	Length, m	Synthesis time, μ s	Synthesis speed, km/s
1	2,929.53	227	12,905	2,830.05	208	13,606
2	2,875.68	215	13,375	2,888.18	215	13,433
3	2,864.61	209	13,706	2,641.66	193	13,687
4	2,774.47	226	12,276	2,592.62	295	8,789
5	3,347.13	274	12,216	2,576.73	189	13,633
6	3,014.34	218	13,827	3,189.65	232	13,748
7	3,067.77	272	11,279	3,149.52	225	13,998
8	2,553.26	190	13,438	2,827.13	205	13,791
9	3,449.78	247	13,967	2,218.31	165	13,444
10	2,394.10	174	13,759	3,569.46	255	13,998
11	3,375.37	312	10,818	2,176.71	169	12,880
12	3,227.03	223	14,471	2,056.36	167	12,314

8. Discussion of results obtained studying the method

The developed method makes it possible to obtain a three-dimensional model of a wire line and its image in real time for any observer location. Synthesis of the geometric model from analytical representation of the line makes it possible to obtain an image of the line for various wire sag values. Such model changes depending on external conditions are impossible or extremely difficult to implement using other methods, in particular lidar scanning and photogrammetry. This is because they ensure only recording of the shape and appearance of the model at some particular time. In this case, the resulting shape itself can have spatial discontinuities. This does not occur when the proposed method is used.

The resulting triangular grid can be directly processed by firmware of the graphical processor. The method can be used in the VS-STC in which a 3D graphics accelerator (available in any modern STC) is used to synthesize images. Also, the method enables obtaining of normals and texture coordinates on the line surface. When synthesizing an

image, this makes it possible to calculate illumination and apply textures to the line surface. This, in turn, increases realism of the synthesized image in general.

The computational resources necessary for the synthesis of the line image are minimized by using switchable detail levels which enables use of cheaper hardware for building a VS and leads to a reduction in the STC costs in general.

The proposed method shortcoming consists in impossibility of direct specifying the number of triangles that form the wire line model. This necessitates dynamic allocation of the graphics accelerator memory to store grids of triangles representing the line. To visualize the line sections distant from the observer, it is necessary to store the α value for each pixel of the synthesized image which requires operation of an additional buffer in the graphics accelerator memory (or an additional channel in the G-buffer).

Filtration according to expression (30) can be used to smooth out edges of vegetation objects or the grass cover and also models rendered by means of a transparency mask, e.g. the detail levels of the power line supports displayed at a considerable distance from the observer.

In the future studies, it is planned to develop methods for modeling emergency and abnormal situations on wire power transmitting lines as well as their visualization in a VS-STC.

9. Conclusions

1. A model of a wire PTL based on the chain line model was considered. Its refinement has been done in such a way that the model has enabled obtaining of a three-dimensional description of the line for VS-STC taking into account distance between supports and the amount of wire sag in real time. The model can be used both for the same and different wire suspension heights.

2. A method has been developed for obtaining a grid of triangles and synthesizing an image of a power transmission line for any observer location in real time. It enables synthesis of a line image using a graphics accelerator. The method also makes it possible to calculate illumination and texturing of the line surface. The number of primitives in the optimized model used to represent the line does not exceed 2 % of the original (for 50 % cases of observation distances). This allows one to minimize necessary computing resources for visualization. In this case, the line parameters can change in real time in contrast to the lidar scanning and photogrammetry methods.

3. Software implementation of the method and study of speed of the process of obtaining geometry and synthesis of line images were carried out. The speed of synthesis of a wire line is more than 13,000 km/s. The obtained results have allowed us to confirm the possibility of applying the method for real-time synthesis of images of lines of various configurations.

References

1. Skarbek L., Zak A., Ambroziak D. Damage detection strategies in structural health monitoring of overhead power transmission system // 7th European Workshop on Structural Health Monitoring. La Cité, Nantes, 2014. P. 663–670.
2. Li L. The UAV intelligent inspection of transmission lines // Proceedings of the 2015 International Conference on Advances in Mechanical Engineering and Industrial Informatics. 2015. doi: <https://doi.org/10.2991/ameii-15.2015.285>
3. Adabo G. J. Long Range Unmanned Aircraft System for Power Line Inspection of Brazilian Electrical System // Journal of Power and Energy Engineering. 2014. Vol. 8, Issue 2. P. 394–398.
4. Arbuzov R. S. Sovremennye metody diagnostiki vozdushnyh liniy elektroperedachi. Novosibirsk: Nauka, 2009. 136 p.
5. Kachanov P. A., Zuev A. A., Yacenko K. N. Space perception analysis in the panini projection and its using in computer graphics // Eastern-European Journal of Enterprise Technologies. 2015. Vol. 4, Issue 2 (76). P. 36–43. doi: <https://doi.org/10.15587/1729-4061.2015.47678>
6. Watts A. C., Ambrosia V. G., Hinkley E. A. Unmanned Aircraft Systems in Remote Sensing and Scientific Research: Classification and Considerations of Use // Remote Sensing. 2012. Vol. 4, Issue 6. P. 1671–1692. doi: <https://doi.org/10.3390/rs4061671>
7. Zhang C., Elaksher A. An Unmanned Aerial Vehicle-Based Imaging System for 3D Measurement of Unpaved Road Surface Distresses // Computer-Aided Civil and Infrastructure Engineering. 2011. Vol. 27, Issue 2. P. 118–129. doi: <https://doi.org/10.1111/j.1467-8667.2011.00727.x>
8. Simulating various terrestrial and UAV LIDAR scanning configurations for understory forest structure modelling / Hämmerle M., Lukač N., Chen K.-C., Koma Z., Wang C.-K., Anders K., Höfle B. // ISPRS Annals of Photogrammetry, Remote Sensing and Spatial Information Sciences. 2017. Vol. IV-2/W4. P. 59–65. doi: <https://doi.org/10.5194/isprs-annals-iv-2-w4-59-2017>
9. Seidel D., Ehbrecht M., Puettmann K. Assessing different components of three-dimensional forest structure with single-scan terrestrial laser scanning: A case study // Forest Ecology and Management. 2016. Vol. 381. P. 196–208. doi: <https://doi.org/10.1016/j.foreco.2016.09.036>
10. UAV Photogrammetry for Mapping and 3D Modeling – Current Status and Future Perspectives / Remondino F., Barazzetti L., Nex F., Scaioni M., Sarazzi D. // ISPRS – International Archives of the Photogrammetry, Remote Sensing and Spatial Information Sciences. 2012. Vol. XXXVIII-1/C22. P. 25–31. doi: <https://doi.org/10.5194/isprsarchives-xxxviii-1-c22-25-2011>
11. Evolutionary View Planning for Optimized UAV Terrain Modeling in a Simulated Environment / Martin R., Rojas I., Franke K., Hedengren J. // Remote Sensing. 2015. Vol. 8, Issue 1. P. 26. doi: <https://doi.org/10.3390/rs8010026>
12. 3D Tree Dimensionality Assessment Using Photogrammetry and Small Unmanned Aerial Vehicles / Gatzliolis D., Lienard J. F., Vogts A., Strigul N. S. // PLOS ONE. 2015. Vol. 10, Issue 9. P. e0137765. doi: <https://doi.org/10.1371/journal.pone.0137765>

13. Panoramic UAV Views for Landscape Heritage Analysis Integrated with Historical Maps Atlases / Brumana R., Oreni D., Alba M., Barazzetti L., Cuca B., Scaioni M. // *Geoinformatics FCE CTU*. 2012. Vol. 9. P. 39–50. doi: <https://doi.org/10.14311/gi.9.4>
14. Liang Y., Qu Y., Cui T. A three-dimensional simulation and visualization system for UAV photogrammetry // *ISPRS – International Archives of the Photogrammetry, Remote Sensing and Spatial Information Sciences*. 2017. Vol. XLII-2/W6. P. 217–222. doi: <https://doi.org/10.5194/isprs-archives-xlii-2-w6-217-2017>
15. Kryukov K. P. *Konstrukcii i mekhanicheskiy raschet liniy elektroperedachi*. 2e izd. Leningrad: Energiya, 1979. 312 p.
16. *Design of Latticed Steel Transmission Structures*. American Society of Civil Engineers. ANSI/ASCE, A.N.S.I. New York: A.S.C.E., 1991. 64 p.
17. Hongnan L., Haifeng B. High-voltage transmission tower-line system subjected to disaster loads // *Progress in Natural Science*. 2006. Vol. 16, Issue 9. P. 899–911. doi: <https://doi.org/10.1080/10020070612330087>
18. Ageev D. M., Bostynec I. P., Didyuk A. Ya. Noviy sposob mekhanicheskogo rascheta provodov i trosov vozdushnyh liniy elektroperedachi // *Vestnik Voronezhskogo gosudarstvennogo tekhnicheskogo universiteta*. 2010.
19. Boshnyakovich A. D. *Mekhanicheskiy raschet provodov i trosov liniy elektroperedachi*. Leningrad: Gosenergoizdat, 1962. 255 p.
20. Issledovaniya provesa provodov LEP, vyzvannogo solnechnym nagrevom / Sotnikova V. N., Solovey P. I., Tanasoglo A. V., Perevaryuha A. N. // *Visnyk Donbaskoi natsionalnoi akademiyi budivnytstva i arkhitektury*. 2015. Issue 3. P. 108–111.
21. Kachanov P. A. Povyshenie tochnosti kodirovaniya normaly dlya sistem vizualizacii, ispol'zuyushchih metod otlozhennogo rascheta osveshcheniya // *Informatsiyno-keruiuchi systemy na zaliznychnomu transporti*. 2012. Issue 6. P. 26–29.